Biochimica et Biophysica Acta 1827 (2013) 689–698

Contents lists available at SciVerse ScienceDirect

Biochimica et Biophysica Acta

journal homepage: www.elsevier.com/locate/bbabio

# Characterization of singlet oxygen production and its involvement in photodamage of Photosystem II in the cyanobacterium *Synechocystis* PCC 6803 by histidine-mediated chemical trapping

Ateeq Ur Rehman, Krisztián Cser, László Sass, Imre Vass *

*Institute of Plant Biology, Biological Research Centre of the Hungarian Academy of Sciences, P. O. Box 521, H-6701 Szeged, Hungary*

ARTICLE INFO

*Article history:*
Received 6 November 2012
Received in revised form 22 February 2013
Accepted 25 February 2013
Available online 4 March 2013

*Keywords:*
Singlet oxygen
Photoinhibition
Photosystem II
Nonradiative charge recombination
Cyanobacteria
*Synechocystis* PCC 6803

ABSTRACT

Singlet oxygen production in intact cells of the cynobacterium *Synechocystis* 6803 was studied using chemical trapping by histidine, which leads to $O_2$ uptake during illumination. The rate of $O_2$ uptake, measured by a standard Clark-type electrode, is enhanced in the presence of $D_2O$, which increases the lifetime of $^1O_2$, and suppressed by the $^1O_2$ quencher $NaN_3$. Due to the limited mobility of $^1O_2$ these data demonstrate that exogenous histidine reaches close vicinity of $^1O_2$ production sites inside the cells. Flash induced chlorophyll fluorescence measurements showed that histidine does not inhibit Photosystem II activity up to 5 mM concentration. By applying the histidine-mediated $O_2$ uptake method we showed that $^1O_2$ production linearly increases with light intensity even above the saturation of photosynthesis. We also studied $^1O_2$ production in site directed mutants in which the Gln residue at the 130th position of the D1 reaction center subunit was changed to either Glu or Leu, which affect the efficiency of nonradiative charge recombination from the primary radical pair (Rappaport et al. 2002, Biochemistry 41: 8518–8527; Cser and Vass 2007, BBA 1767:233–243). We found that the D1-Gln130Glu mutant showed decreased $^1O_2$ production concomitant with decreased rate of photodamage relative to the WT, whereas both $^1O_2$ production and photodamage were enhanced in the D1-Gln130Leu mutant. The data are discussed in the framework of the model of photoinhibition in which $^3$P680 mediated $^1O_2$ production plays a key role in PSII photodamage, and nonradiative charge recombination of the primary charge separated state provides a photoprotective pathway.


## 1. Introduction

Photosynthesis is driven by light, which can be highly energetic and potentially dangerous substance that can damage the photosynthetic apparatus (for a historical overview see Ref. [1]). The light-induced decline of photosynthetic activity is broadly termed as photoinhibition, and this important phenomenon has been a topic of intense research in the last 30 years. The major site of photoinhibition is the Photosytem II (PSII) complex whose electron transport is inhibited and protein structure is damaged as a consequence of light exposure (see Ref. [2] for a review).

Although significant efforts have been devoted to clarify the mechanisms of photoinhibition of PSII no consensus has been reached yet and different models are considered to explain the detrimental effects of visible light on PSII (for recent reviews see [3–7]). These models include: (i) Modifications in the functioning of the $Q_B$ [8] and $Q_A$ acceptors [9–11] under conditions of excess excitation when the capacity of secondary metabolic processes is not sufficient to utilize the electrons produced in the primary photoreactions. (ii) Charge recombination processes that result in triplet Chl formation [12] and their involvement in subsequent singlet oxygen production in the PSII reaction center [9,11,13–16]. (iii) Visible light induced direct damage of catalytic Mn complex of water oxidation has also been suggested [17,18], and it is known from EPR studies that spin state changes in the Mn cluster can be induced by light at the far-red edge of the visible range [19].

Singlet oxygen ($^1\Delta_gO_2$, which will be abbreviated as $^1O_2$) is produced via interaction of ground state molecular oxygen ($^3\Sigma_gO_2$) with Chl triplets in PSII, and has been implicated in the process of photoinhibition as an important mediator of light induced damage. Production of $^1O_2$ has been demonstrated in isolated PSII reaction center complexes by histidine- or imidazole mediated chemical trapping [20], and also by direct 1270 nm luminescence measurements

*Abbreviations:* Chl, chlorophyll; D1 and D2, reaction center protein subunits of Photosystem-II; DanePy, 3-[N-(b-diethylaminoethyl)-N-dansyl]aminomethyl-2,2,5,5-tetramethyl-2,5-dihydro-1H-pyrrole; DCMU, 3-(3′,4′-dichlorophenyl)-1,1-dimethylurea; NPQ, non-photochemical quenching; PQ and PQH2, plastoquinone and plastoquinol, respectively; PSII, Photosystem-II; P680, reaction center Chl; OCP, orange carotenoid protein; ROS, reactive oxygen species; SOD, superoxide dismutase; SOSG, Fluorescence Sensor Green; TEMP, 2,2,6,6-tetramethylpiperidine; TEMPD-HCl, 2,2,6,6-tetramethyl-4-piperidone hydrochloride

* Corresponding author. Tel.: +36 62 599 700; fax: +36 62 433 434.
*E-mail address:* vass.imre@brc.mta.hu (I. Vass).

0005-2728/$ – see front matter © 2013 Elsevier B.V. All rights reserved.
http://dx.doi.org/10.1016/j.bbabio.2013.02.016

[21,22]. In thylakoid membrane particles EPR spin trapping was applied successfully for $^1O_2$ detection by using either TEMP [15,23,24], or TEMPD-HCl [25], see also Ref. [26] for a recent summary of the method. The direct 1270 nm luminescence measurements could also be used in isolated PSII complexes [27]. In intact plant systems the fluorescent $^1O_2$ traps DanePy [28,29] and Fluorescence Sensor Green (SOSG) have been applied [30]. However, detection of singlet oxygen production in intact cyanobacterial cells presents a significantly larger challenge since the EPR and fluorescent spin traps do not penetrate inside the cells (E. Hideg, personal communication), and application of the direct 1270 nm luminescence method is hampered by the influence of background Chl fluorescence [31]. It is of note that there has been an attempt to use SOSG in intact *Synechocystis* cells [32]. However the requirement of long illumination under photonhibitory conditions (3 h at 1000 μmol quanta $m^{-2}$ $s^{-1}$) for the induction of the SOSG fluorescence signal [32] together with $^1O_2$ production by illuminated SOSG itself, which induces an artifactual fluorescence increase in the absence of exogenous singlet oxygen source [33] limits the applicability of this method for quantitative detection of singlet oxygen in *Synechocystis*.

Here we describe in detail the applicability of histidine mediated chemical trapping for the detection of $^1O_2$ in intact *Synechocystis* 6803 cells, and demonstrate that $^1O_2$ production linearly depends on light intensity. We also show that the efficiency of $^1O_2$ production is modulated by amino acid replacements at the 130th position of the D1 protein, which modifies the redox potential of Phe and affects the efficiency of non-radiative charge recombination of the primary radical pair. The presented results provide support for the photoprotective role of non-radiative charge recombination processes in the PSII reaction center.

## 2. Materials and methods

### 2.1. Cell cultures

*Synechocystis* sp. PCC 6803 (which will be referred to as *Synechocystis*) cells were propagated in BG-11 growth medium in a rotary shaker at 30 °C under a 3% $CO_2$-enriched atmosphere. The intensity of white light during growth was 40 μmol quanta $m^{-2}$ $s^{-1}$. Cells in the exponential growth phase ($A_{580}$ of 0.8–1) were used. The D1-Gln130Leu and D1-Gln130Glu mutants were constructed in the *psbA3* gene of *Synechocystis* sp. PCC 6803 by Peter Nixon as described previously [34].

### 2.2. Light treatment

Cells were harvested by centrifugation at 8000 *g* for 5 min and resuspended in 100 mL fresh BG-11 medium at 5 μg Chl $mL^{-1}$ concentration. Before starting high light treatment cells were left for 1 h under 40 μmol quanta $m^{-2}$ $s^{-1}$ light at continuous stirring followed by a measurement of the control value of oxygen evolution, which was used as zero time point for the high light treatment. For photoinhibitory treatment cells were illuminated with 500 μmol quanta $m^{-2}$ $s^{-1}$ light in the presence of the protein synthesis inhibitor lincomycin (300 μg/ml).

### 2.3. Variable fluorescence measurements

Flash-induced increase and the subsequent decay of chlorophyll fluorescence yield was measured by a double-modulation fluorometer (PSI Instruments, Brno) [35] in the 150 μs to 100 s time range as described earlier [36]. The sample concentration was 5 μg Chl/ml. The same instrument was used for the measurement of variable fluorescence under continuous illumination by using the so called OJIP protocol.

### 2.4. Oxygen evolution measurements

Oxygen evolution for quantification of light induced loss of PSII activity was measured with a Hansatech DW2 $O_2$ electrode at saturating light intensity in the presence of 0.5 mM DMBQ, as an artificial electron acceptor. 2 mL of cells at 5 μg Chl $mL^{-1}$ was used in each measurement, and three replicates were measured.

### 2.5. Histidine mediated oxygen uptake measurements

$^1O_2$ production in cell free BG-11 medium was initiated by illumination in the presence of 1 μM Rose Bengal (RB). $^1O_2$ was detected by measuring the rate of light induced oxygen uptake in the presence of 5 mM histidine. For the enhancement of $^1O_2$ production $H_2O$ was replaced with $D_2O$ in BG-11, while quenching of $^1O_2$ was achieved by the addition of 10 mM $NaN_3$. The effect of further reactive oxygen species on His-mediated oxygen uptake was probed by oxygen measurements in BG-11 medium containing 5 mM His in the presence of 500 μM $H_2O_2$, or artificially generated hydroxyl radials (500 μM $H_2O_2$ + 200 μM $Fe(NH_4)_2(SO_4)_2$), or artificially generated superoxide (100 μM xanthine + 0.025 unit/ml xanthine oxidase [37,38]).

Singlet oxygen production in intact cells was detected by measuring the rate of light induced oxygen uptake in the presence of 5 mM His as described earlier for isolated PSII reaction center complexes [20]. *Synechocystis* cells were centrifuged and resuspended in fresh BG-11 medium before $O_2$ uptake measurements, which were performed by using a Hansatech DW2 $O_2$ electrode in the absence of artificial electron acceptors.

### 2.6. Simulation of PSII electron transport

Light induced accumulation of $Q_A^-$ as well as $^3$P680 was simulated on the basis of a coupled differential equation system describing 18 different states of PSII based on the electron transport network shown in Scheme 1 (see below). For the sake of simplicity some rarely populated states are omitted from Scheme 1 although they were considered for the calculations. The equations were solved numerically by using MATLAB with the rate constants shown in Table I of the Supplementary material.

## 3. Results and discussion

In order to establish a method that can be applied for detection of $^1O_2$ production in intact *Synechocystis* cells we used a chemical trapping method in which a good singlet oxygen acceptor, such as histidine (or imidazole) reacts with $^1O_2$ [39]. This reaction occurs via the addition of the singlet oxygen molecule to the imidazole ring to yield short-lived peroxide species and leads to incorporation of oxygen into oxidized endproducts (see Refs. [40,41]). This process removes dissolved $O_2$ from the cell suspension in a $^1O_2$-concentration dependent way, which effect can be easily quantified by oxygen uptake measurements by using a standard oxygen electrode.

### 3.1. His-mediated $O_2$ uptake reflects $^1O_2$ production in cell free culture medium

As shown in Fig. 1A the $O_2$ level was not affected by illumination in the BG11 medium in the presence of 5 mM His alone (closed circles). When BG11 was supplemented with Rose Bengal (RB), which is a strong sensitizer of light induced $^1O_2$ production, switching on the light induced a rapid $O_2$ uptake in the presence of His, which is due to the removal of dissolved $O_2$ by His-mediated $^1O_2$ trapping (Fig. 1A, down triangles). It is of note that a small light induced decrease of the $O_2$ level was also observed when RB was added without His (up triangles). This effect is most likely the consequence of $^1O_2$ trapping by organic ingredients of BG11.

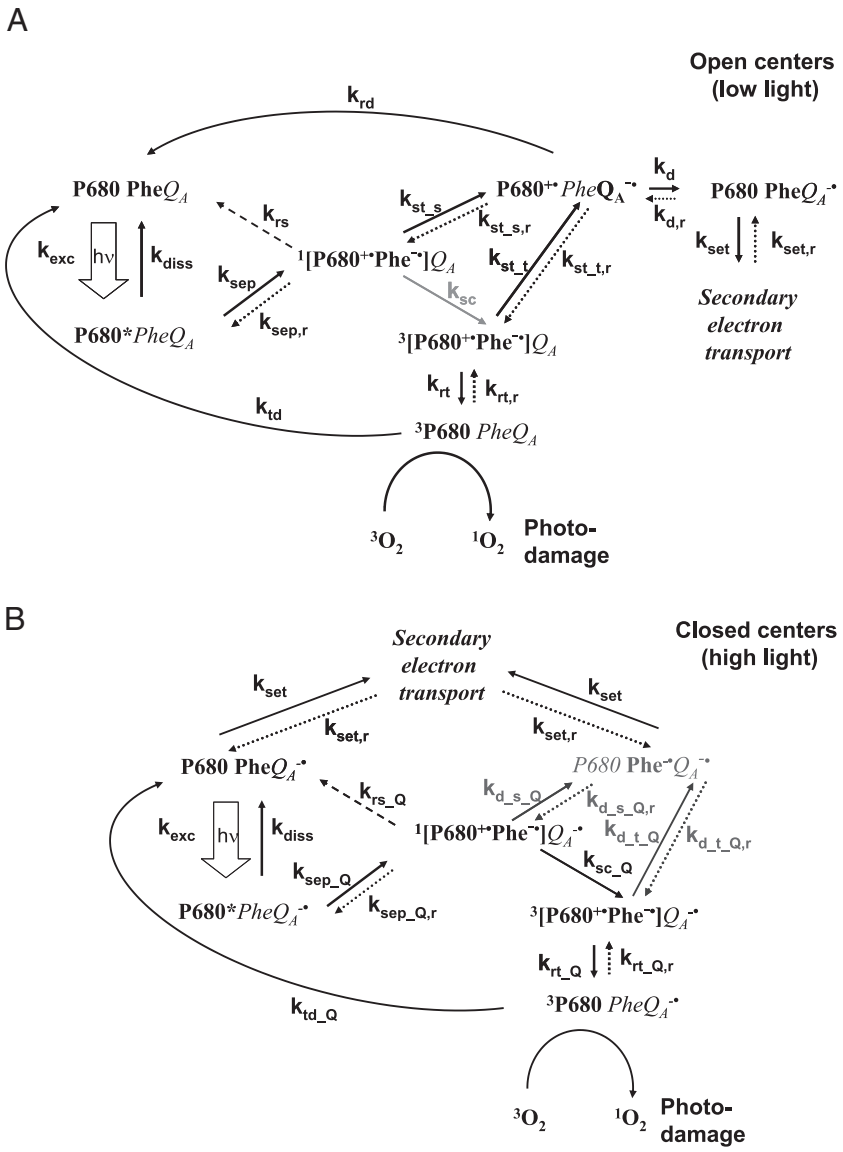


**Scheme 1.** Main pathways of electron transport in PSII in relation to $^3$P680 formation and $^1O_2$ production. Panels A and B of the scheme show events that occur in the presence of initially oxidized and reduced $Q_A$, i.e. in open and closed PSII centers, which are characteristic for low and high light conditions, respectively. In open PSII centers the following processes are considered (when appropriate the reverse processes are also shown with an *r* subscript in the rate constants): Light induced excitation of P680 ($k_{exc}$); Initial charge separation ($k_{sep}$); Direct recombination of the singlet primary charge pair ($k_{rs}$); Stabilization of the singlet primary charge pair via reduction of $Phe^-$ by $Q_A$ ($k_{st\_s}$); Elimination of the $P680^{+\bullet}Q_A^{-\bullet}$ state via direct recombination ($k_{rd}$), as well as via reverse electron flow to the singlet and triplet primary charge pair ($k_{st\_s,r}$ and $k_{st\_t,r}$, respectively); Spin conversion of the singlet primary charge pair into its triplet form ($k_{sc}$); Stabilization of the triplet primary charge pair via reduction of $Phe^-$ by $Q_A$ ($k_{st\_t}$); Recombination of the triplet primary charge pair to $^3$P680 ($k_{rt}$) followed by its decay to the ground state directly ($k_{td}$), or via $^1O_2$ production; Stabilization of the $P680^{+\bullet}Q_A^{-\bullet}$ state via electron donation from PSII donors to $P680^{+\bullet}$ ($k_d$); Secondary electron transport from $Q_A^-$ to $Q_B$ and the PQ pool, as well as from water to oxidized PSII donors ($k_{set}$). The processes that occur in closed PSII centers are basically the same as in the open PSII, but have different rate constants, which are indicated with Q in the subscript. The main difference is that in the closed centers stabilization of the primary charge pair can occur only via electron donation from PSII donors to $P680^{+\bullet}$ both in the singlet and triplet configuration of the ($k_{d\_s\_Q}$ and $k_{d\_t\_Q}$). Closed centers can be converted to open centers after partial oxidation of the PQ pool allowing the oxidation of $Q_A^-$ via $Q_B$ or $Q_B^-$.

The correlation of His-mediated $O_2$ uptake with $^1O_2$ trapping was further confirmed by adding $NaN_3$, which is a $^1O_2$ quencher (see Ref. [42]), and suppressed the $O_2$ uptake effect (Fig. 1A, open circles). Furthermore, addition of $D_2O$, which extends the lifetime of $^1O_2$ [43,44] and therefore increases the probability for its trapping by His, enhanced the rate of $O_2$ uptake (open squares). The calculated $O_2$ uptake rates confirm that the presence of $D_2O$ significantly enhances the rate of His-mediated oxygen removal, whereas $NaN_3$ almost completely eliminates it (Fig. 1A inset). Another $^1O_2$ sensitizer, methylene blue, was also applied which led essentially to the same results as RB (not shown). The above data demonstrate that His-mediated chemical trapping can be applied for $^1O_2$ detection in BG11 containing media.

Since His may also react with reactive oxygen species other than $^1O_2$ we checked the effect of $H_2O_2$, hydroxyl radicals and superoxide on the level of dissolved oxygen in the presence of His. As shown in Fig. 1B, the addition of 0.5 mM $H_2O_2$ in the presence of 5 mM His did not induce any oxygen uptake (Fig. 1B, full circles). Hydroxyl radicals, which were produced via the Fenton reaction by mixing 0.5 mM $H_2O_2$ + 200 μM $Fe^{2+}$ added in the form of $Fe(NH_4)_2(SO_4)_2$, did not lead to His mediated $O_2$ uptake either (Fig. 1B, full triangles). Production of superoxide by mixing 100 μM xanthine + 0.025 unit/ml xanthine oxidase [37,38] induced an $O_2$ uptake effect by converting $O_2$ to $O_2^-$ (Fig. 1B, open diamonds). However, the $O_2$ uptake was not affected by the addition of His together with xanthine and xanthine oxidase (Fig. 1B closed diamonds). These data show that the presence of $H_2O_2$, hydroxyl radicals, or superoxide is not expected to induce His mediated $O_2$ uptake that would compromise the effect arising from the trapping of $^1O_2$.

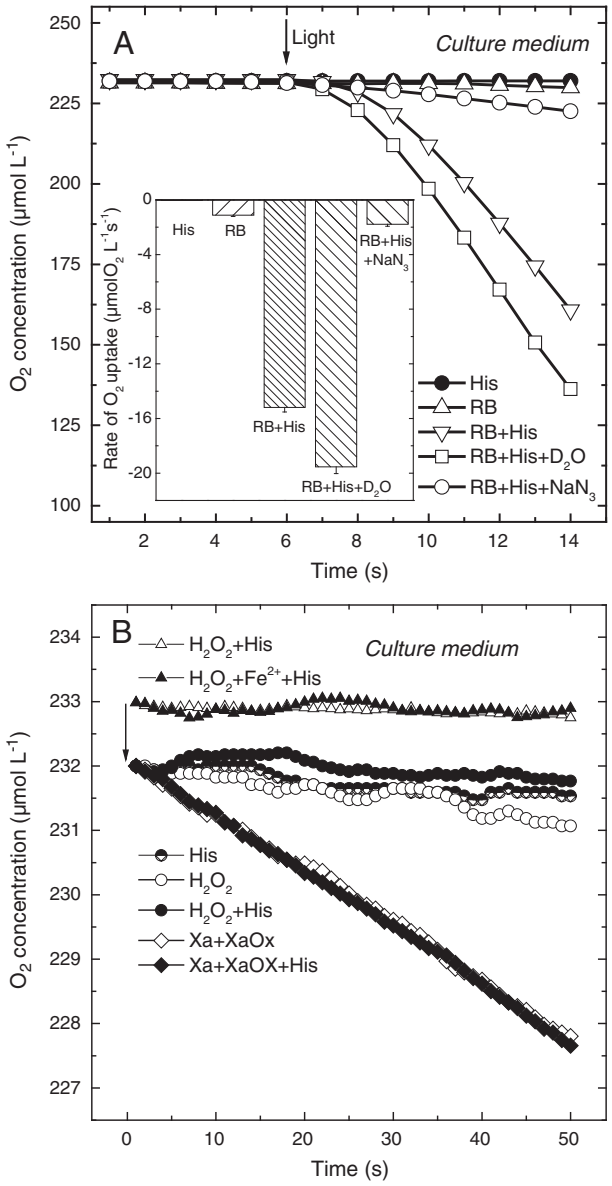


**Fig. 1.** His-dependent oxygen uptake in BG11 culture medium. A, Concentration changes of dissolved oxygen were measured by a Clark type oxygen electrode in cell free BG11 culture medium in the presence of 5 mM His (closed circles), 1 μM Rose Bengal (RB) (up triangles), 5 mM His + 1 μM RB (down triangles), 5 mM His + 1 μM RB in $D_2O$ containing BG11 (squares), 5 mM His + 1 μM RB + 10 mM $NaN_3$ (open circles). The light intensity was 2300 μmol quanta $m^{-2}$ $s^{-1}$. The inset shows rates of oxygen uptake calculated from traces like those shown in the presence of His, RB, RB + His, RB + His + $D_2O$, and RB + His + $NaN_3$. The data represent mean values from 3 independent measurements with the indicated errors. B, Oxgen uptake measurements were performed in the dark in the presence of 500 μM $H_2O_2$ (open circles), 5 mM His (half-closed circles), 500 μM $H_2O_2$ + 5 mM His (closed circles), 100 μM xanthine + 0.25 unit/mL xanthine oxidase (open diamonds), 100 μM xanthine + 0.25 unit/mL xanthine oxidase (open diamonds) + 5 mM His (closed diamonds). In a separate experiment the effect of 500 μM $H_2O_2$ + 200 μM $Fe^{2+}$ (added in the form of $Fe(NH_4)_2(SO_4)_2$) + 5 mM His was also checked (closed triangles). This curve is shown together with its 500 μM $H_2O_2$ + 5 mM control (open triangles). For the sake of clarity the $H_2O_2$ + His, and $H_2O_2$ + His + $Fe^{2+}$ curves are shown after shifting along $O_2$ concentration axis by 1 μmol $O_2L^{-1}$. The actual position of these curves is shown by the arrow.

### 3.2. His-mediated $O_2$ uptake reflects $^1O_2$ production in intact Synechocystis cells

An important prerequisite of $^1O_2$ trapping in intact cells is that the trap molecules should reach cell compartments where $^1O_2$ is produced. Due to their short lifetime the mobility of $^1O_2$ molecules is very limited (ca. 200 nm in water and 400 nm in membranes [45]), which prevents their migration from the cells to the external medium. Therefore, the observation that His induces light dependent $O_2$ uptake in the suspension of *Synechocystis* cells (see below in Fig. 3), while it has no effect in cell free BG11 medium (Fig. 1A) shows that exogenous His penetrates inside the cells reaching close vicinity of the site of $^1O_2$ production.

A further requirement for the applied trap is that it should not inhibit PSII electron transport activity, which could influence $O_2$ production and therefore lead to a misleading calculation of singlet oxygen production. Such an effect would represent an artifact in the $O_2$ uptake measurements in *Synechocystis* cells, which produce $O_2$ themselves during illumination. The effect of exogenously added His on PSII was assessed by flash induced variable Chl transients, which reflect the functioning of electron transport both at the donor and acceptor side of PSII. Illumination of *Synechocystis* cells with a single turnover saturating flash reduces the $Q_A$ acceptor, which leads to increased fluorescence yield (Fig. 2A). Subsequent reoxidation of $Q_A^-$ in the dark results in the relaxation of fluorescence yield exhibiting three main decay phases. The two faster decay components reflect the reoxidation of $Q_A^-$ by PQ molecules which are already bound to the $Q_B$ site at the time of the flash ($\tau$ ~ 500–600 μs) or bind from the PQ pool after the flash ($\tau$ ~ 5–10 ms), respectively [46]. Whereas, the slow phase of the decay ($\tau$ ~ 10–15 s) arises from back reaction of the $S_2$ state of the water-oxidizing complex with $Q_A^-$, which is populated via the equilibrium between $Q_A^-Q_B$ and $Q_AQ_B^-$ ([47,48]). In the presence of DCMU, which blocks the $Q_B$ binding site the fluorescence relaxation occurs via recombination of $Q_A^-$ with oxidized PSII donors components and the process is dominated by the $S_2Q_A^-$ recombination [48].

It is clear from Fig. 2A. that neither the amplitude nor the kinetics of the fluorescence signal is affected at 5 mM His concentration, in the absence or presence of DCMU. As a consequence His does not induce modification of PSII electron transport at the level of the $Q_A$ and $Q_B$ quinone electron acceptors, or the water oxidizing complex. However, at higher concentrations (above 10 mM) His addition induces a small decrease in the amplitude of flash induced Chl fluorescence relaxation traces (not shown), which shows that exogenously added His can reach the immediate vicinity of the PSII complex, or its antenna. The so called OJIP variable Chl fluorescence transient, which reflects the efficiency of electron transfer from the water oxidizing complex to the acceptor side of PSII, was also measured. Again, this variable fluorescence transient was not affected by 5 mM His either in the absence or presence of DCMU (Fig. 1B). Based on these data we can conclude that up to 5 mM concentration His does not interfere with PSII activity and potentially suitable for $^1O_2$ trapping in intact *Synechocystis* cells.

The $^1O_2$ quencher $NaN_3$ is known to affect photosynthetic activity and expected to decrease the rate of oxygen evolution (see [49]), which would interfere with the $O_2$ uptake assay if it is applied in cells with functional oxygen evolving activity. Therefore, $NaN_3$ was applied in the presence of DCMU, which blocks the $Q_B$ site and eliminates $O_2$ evolution. As shown in Fig. 2B addition of 10 mM $NaN_3$ induced a decrease of variable fluorescence in the presence of DCMU showing a partial inhibition of PSII activity. However, this effect is not expected to interfere significantly with the His mediated $O_2$ uptake when performed in the presence of DCMU (see below).

We have also tested the effect of imidazole, which was used earlier as a chemical trapping agent for $^1O_2$ detection in isolated PSII reaction center complexes [20]. However, in contrast to histidine 5 mM imidazole induced a significant inhibition of PSII activity as revealed by the decreased amplitude and retarded relaxation kinetics of the flash induced Chl fluorescence traces, as well as by the decreased induction of the OJIP fluorescence transient (not shown). The mechanism of this inhibitory effect of PSII activity by imidazole is not clear at present, and we restricted our studies to using His as chemical $^1O_2$ trap.

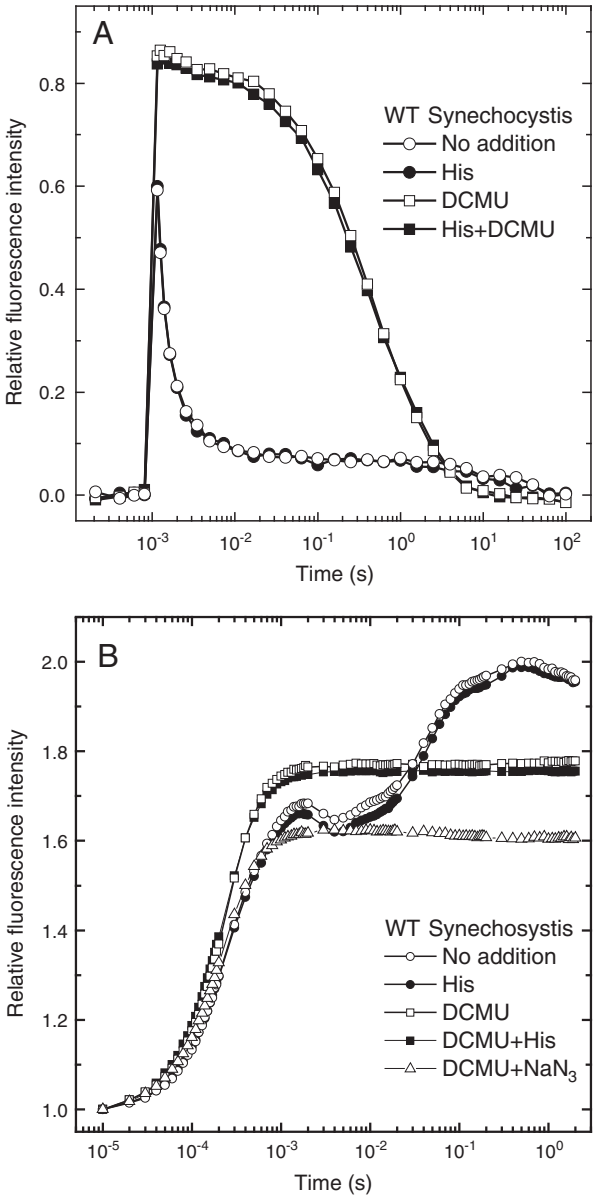


**Fig. 2.** Effect of histidine addition on variable fluorescence characteristics of *Synechocystis* cells. A, Flash induced Chl fluorescence traces in the absence (open symbols) and presence of 5 mM His (closed symbols). The curves, which were measured either without electron transport inhibitor (circles), or in the presence of 10 μM DCMU (squares) are shown after shifting them to the same initial Fo fluorescence level. B, Variable Chl fluorescence traces in the absence (open symbols) and presence of 5 mM His (closed symbols). The traces were measured either without electron transport inhibitor (circles), or in the presence of 10 μM DCMU (squares and triangles). The effect of 10 mM $NaN_3$ is shown in the presence of DCMU (triangles). The curves are presented after shifting them to same initial Fo fluorescence level.

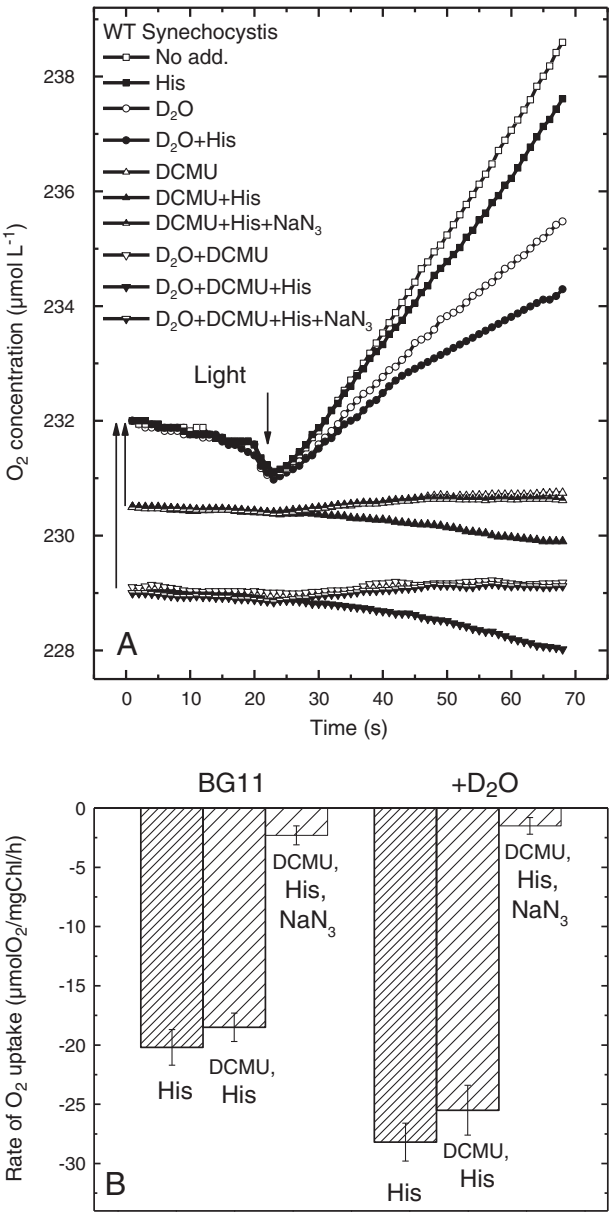


**Fig. 3.** Effect of $D_2O$ and sodium azide on His-mediated $O_2$ uptake in *Synechocystis*. A, Light induced changes in the concentration of dissolved oxygen were followed in *Synechocystis* cell suspensions containing $H_2O$ (squares and up triangles) or $D_2O$ (circles and down triangles) in the absence (open symbols), and in the presence of 5 mM His (closed, and half closed symbols). The measurements were also performed in the presence of 10 μM DCMU (triangles) where the effect of 10 mM $NaN_3$ in the presence of 5 mM His was also tested (half closed symbols). Light intensity during the oxygen measurements was 2300 μmol quanta $m^{-2}$ $s^{-1}$. For the sake of clarity some curves are shown after shifting along $O_2$ concentration axis. The actual position of these curves is shown by the arrow. B, Rate of His-mediated $O_2$ uptake in $H_2O$ and $D_2O$ containing cell suspensions. The data are mean values from 3 measurements performed at 2300 μmol quanta $m^{-2}$ $s^{-1}$ light intensity with the indicated errors.

When the effect of 5 mM His was checked on the $O_2$ evolving activity of *Synechocystis* cell cultures no modification of the rate of dark respiration was observed, in contrast the apparent rate of light induced oxygen evolution was decreased (Fig. 3A, open and closed squares). Since inhibition of PSII electron transport does not occur at this His concentration (see above, Fig. 2), the apparent decrease of the $O_2$ evolution rate indicates that His induces an $O_2$ removal process from the cell suspension. This process is in competition with light induced oxygen evolution and can be related to His-mediated $^1O_2$ trapping. This hypothesis was verified by using $D_2O$ in the suspension medium instead of $H_2O$, which extends the lifetime of $^1O_2$ [43,44] and therefore enhances the probability of $^1O_2$ trapping by His (Fig. 3A, open and closed circles). Although $D_2O$ in itself decreased the rate of $O_2$ evolution the extent of $O_2$ uptake by His addition was clearly increased relative to that obtained in the $H_2O$ containing medium (Fig. 3B), which supports the idea that His-mediated $O_2$ uptake reflects $^1O_2$ trapping.

Further support for the idea that His-mediated $O_2$ uptake arises from $^1O_2$ trapping is provided by the observation of real $O_2$ uptake in the presence of DCMU, which blocks $O_2$ evolution by occupying the $Q_B$ binding site. When only DCMU was added to the *Synechocystis* cells light induced increase in the level of dissolved oxygen was almost completely eliminated (Fig. 3A, open op triangles). The apparent small residual $O_2$ evolution could arise from the non-complete inhibition of

PSII activity by the applied 10 μM DCMU. However, this effect must be very small since the flash induced fluorescence relaxation curves (Fig. 2A) and steady state variable fluorescence transients (Fig. 2B) show a large extent inhibition of electron transport at the acceptor side of PSII. Another reason for the apparent residual $O_2$ evolution in the presence of DCMU could be a light induced decrease in the rate of respiration, as was shown earlier for another cyanobacterium *Trichodesmium* spp. by membrane inlet mass spectrometry, which effect was assigned to partial diversion of electrons that would end up at the terminal oxidase(s) in the dark towards $NADP^+$ in the light via PSI [50]. The rate of respiration in the presence of DCMU is apparently smaller than in the absence of this inhibitor. This effect most likely arises from the usage of different cell culture batches for the measurements, which were performed in the absence and presence DCMU. We did not observe DCMU affect on the respiration rate when the measurements were performed in the same cell culture with and without DCMU (not shown). The previous membrane inlet mass spectrometry data did not show DCMU effect on the respiration rate either [50]. Illumination in the presence of DCMU + His an absolute $O_2$ uptake was observed (Fig. 2A, closed up triangles), which effect was enhanced in the presence of $D_2O$ (Fig. 2A, closed down triangles) in agreement with the increased lifetime of $^1O_2$ in $D_2O$. These observations confirm that His-mediated $O_2$ uptake in intact *Synechocystis* cells in the absence of DCMU cannot be caused by a small inhibition of $O_2$ evolution by His addition, which may cause such a small extent of change in the variable fluorescence characteristics in Fig. 2 that is masked by experimental error.

Based on these findings DCMU inhibition of $O_2$ evolution could be a standard part of the His-mediated $O_2$ uptake measurement protocol. However, electron transport inhibitors, which act at the $Q_B$ site modify the redox potential of $Q_A$ and influence charge recombination pathways in PSII and modify $^1O_2$ production efficiency [51,52]. Such an effect may interfere with the modifications of charge recombination characteristics induced by the studied mutations (see below). Therefore, we prefer to perform the $O_2$ uptake measurements without DCMU unless other treatments, such as $NaN_3$, induce partial inhibition of $O_2$ evolution which should be masked by complete inhibition of $O_2$ evolving activity.

Further support for $^1O_2$ trapping by His comes from the suppression of $O_2$ uptake in the presence of the $^1O_2$ quencher $NaN_3$. Since $NaN_3$ inhibits $O_2$ evolution [49] its $^1O_2$ quenching effect was tested in the presence of DCMU where the artifact that would arise from the decreased of $O_2$ evolution rate could be avoided. Addition of $NaN_3$ almost completely reversed $O_2$ uptake either in $H_2O$, or $D_2O$ containing cell suspensions (Fig. 3A, half closed up and down triangles, respectively).

It has to be noted that $NaN_3$ causes a partial inhibition of PSII activity even in the presence of DCMU (Fig. 2B). However, this inhibitory effect is not expected to eliminate $^1O_2$ production, which can be observed even in isolated PSII reaction center complexes that lack completely $O_2$ evolving activity [20]. It is also of note that $NaN_3$ is not only a $^1O_2$ quencher, but also an inhibitor of SOD [53] and catalase [49]. Therefore, $NaN_3$ addition could lead to accumulation of $O_2^-$ and/or $H_2O_2$ in the cells besides quenching $^1O_2$. However, it is highly unlikely that this effect could cause an artifact that would be responsible for the observed elimination of His-mediated $O_2$ uptake in the presence of $NaN_3$ as observed in Fig. 3 since our data show that neither $O_2^-$, nor $H_2O_2$ interacts with His (Fig. 1B) that would modify the level of dissolved $O_2$. Therefore, the $NaN_3$ induced elimination of His-mediated $O_2$ uptake in the presence of DCMU provides strong support for the idea that the $O_2$ uptake effect is indeed due to $^1O_2$ trapping by His.

Based on the above presented key observations, which show that illumination in the presence of His induces $O_2$ uptake both in the absence and presence of DCMU, that is enhanced by $D_2O$ and suppressed by $NaN_3$ we can conclude that His at 5 mM concentration is a suitable chemical trap for $^1O_2$ detection in intact *Synechocystis* cells.

### 3.3. $^1O_2$ production is linearly dependent on light intensity

The production of singlet oxygen in photosynthetic systems involves the formation of triplet Chl states in the PSII reaction center, or in the light harvesting antenna (see Refs. [4,54,55]). This is followed by the interaction of Chl triplets with molecular $O_2$, which also has triplet configuration in its ground state, and leads to the formation of highly reactive $^1O_2$. Since the amount of $O_2$ is usually high in comparison with the amount of Chl triplets the yield of $^1O_2$ production is limited by the availability of $^3$Chl. On the other hand, the amount of Chl triplets is expected to be linearly dependent on light intensity not only in the light harvesting antenna, but also in the case of the PSII reaction center Chl P680 (see discussion below). Therefore, the yield of $^1O_2$ production is expected to be linearly increasing with increasing light intensity. This expectation has been supported earlier in isolated PSII membranes by using EPR spin trapping [56]. The hypothesis that light intensity dependence of $^1O_2$ production can be followed by His-mediated $O_2$ uptake was tested in an *in vitro* system of BG11 medium and Rose Bengal as $^1O_2$ sensitizer, which indeed showed linear light intensity response in the 34–2300 μmol quanta $m^{-2}$ $s^{-1}$ intensity range (not shown).

In photosynthetic systems most of the $^1O_2$ production is expected to arise from the triplet state of the P680 reaction center Chl assembly. $^3$P680 is produced via charge recombination from the triplet charge separated state ($^3$ [$P680^{+\bullet}Phe^{-\bullet}$]) whose amount is determined by the competition of spin conversion and forward electron transport from the singlet charge separated state ($^1$ [$P680^{+\bullet}Phe^{-\bullet}$]), as well as of reverse electron flow from the $P680^{+\bullet}PheQ_A^{-\bullet}$ state to the singlet and triplet charge separated states (Scheme 1).

In low light, when secondary electron transport toward $CO_2$ fixation and other light-independent processes (such as the water–water cycle and chlororespiration) are able to utilize the electrons which are liberated from water by the primary charge separation event, $Q_A$ is mainly oxidized, and PSII is in the so called open state. Under these conditions charge stabilization via forward electron transport from $Phe^-$ to $Q_A$ can compete efficiently with spin conversion, therefore reverse electron flow from $P680^+\bullet PheQ_A^-\bullet$ to $^3$ [$P680^+\bullet Phe^-\bullet$]$Q_A$ is the main source of $^3$P680 formation in low light (Scheme 1A.). With the increase of light intensity the electron transport chain will be gradually reduced, which stabilizes $Q_A^-\bullet$ and converts PSII into the so called closed state. Under these conditions the newly formed primary radical pair can be stabilized only via electron donation to $P680^+\bullet$ from secondary PSII donors (Scheme 1B). This process has a low rate (ca. $4*10^6$ – $2*10^7$ $s^{-1}$ depending on the oxidation state of the water-oxidizing complex [57]) relative to that of spin conversion (ca. $3 * 10^8$ [58]). If the rate constant of primary charge separation and the stability of $^3$P680 would remain the same in the closed PSII centers as in the open centers the above processes would drastically enhance the yield of the $^3$P680 forming pathway as can be observed in isolated PSII reaction center complexes, which lack $Q_A$, or have doubly reduced $Q_A$ that is neutralized by protonation [59]. Based on picosecond fluorescence and absorption change measurements the rate of charge separation and the yield of primary radical formation are expected to decrease by a factor of 2–3 in the presence of fully reduced $Q_A$ [60]. Parallel EPR and flash absorption spectroscopy measurements also showed an ≈2-fold decrease in the yield of primary radical pair formation [59]. In addition a significant, ca. 100-fold, acceleration of the decay of $^3$P680 was observed in the presence of $Q_A^-\bullet$ in cryogenic temperatures [59] from which an accelerated decay of $^3$P680 can also be predicted at room temperature in closed PSII centers. Therefore, the decreased yield of primary charge pair formation can partly compensate the increase, which is expected to occur in the yield of $^3$P680 due PSII closure. In addition, the accelerated decay of $^3$P680 decreases the probability that $^3$P680 can interact with $O_2$. These effects together partly compensate

the potential for the increase in the yield of $^1O_2$ in closed PSII centers, which however is expected to be still higher than in open PSII. Since the rate of primary charge separation is light intensity dependent the steady state level of $^3$P680 should increase with increasing light intensities in closed PSII centers, even if the yield of $^3$ [$P680^+$•$Phe^-$•] formation is low and $^3$P680 decay is accelerated in the presence of $Q_A^-$ leading to light intensity dependent increase of $^1O_2$.

A computer simulation on the basis of Scheme 1. using the rate constants shown in Table I of the Supplementary material indeed shows that the concentration of $^3$P680 increases linearly in a wide intensity range even after $Q_A$ is fully reduced (Fig. 4A). This prediction could also be verified experimentally when $^1O_2$ production was measured in a suspension of intact *Synechocystis* cells and yielded linear light intensity dependence in the 30–2300 μmol quanta $m^{-2}$ $s^{-1}$ range (Fig. 4B).

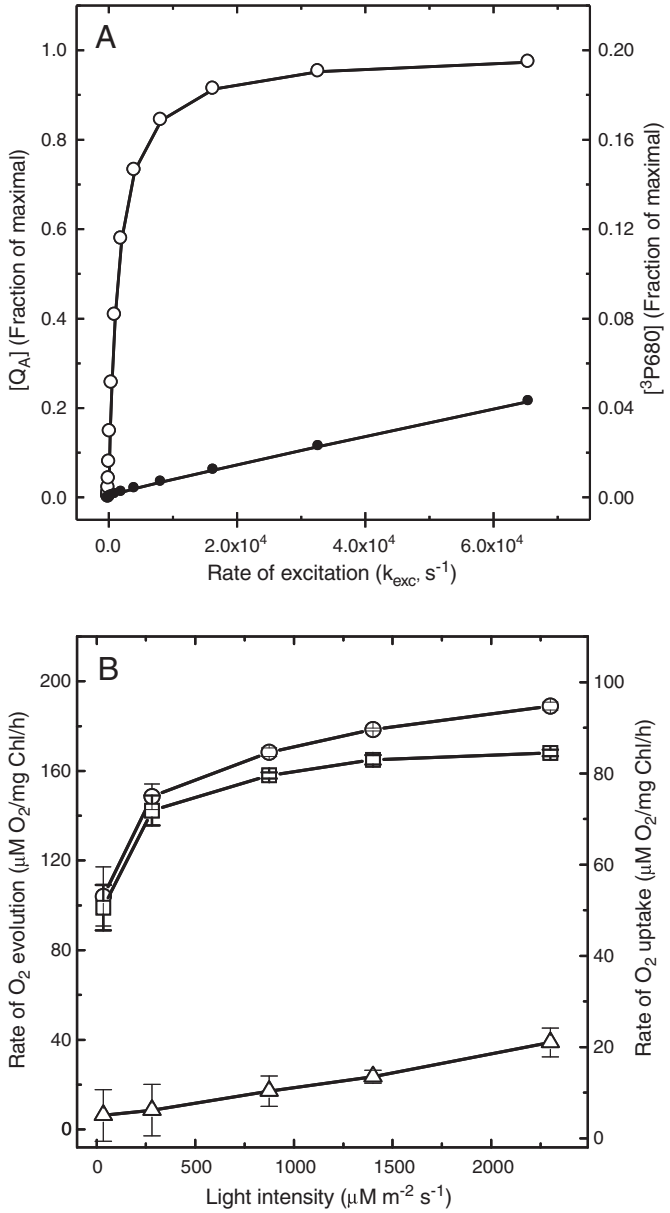


**Fig. 4.** Light intensity dependence of $^3$P680 formation and singlet oxygen production. A, Light induced changes in the amount of $Q_A^-$ and $^3$P680 were calculated by using a differential equation system based on Scheme 1 and the rate constants in Table I of the supplementary material. The fraction of PSII centers with $Q_A^-$ (open circles) and with $^3$P680 (closed circles) are plotted as a function of the rate of excitation, which is proportional with light intensity. B, Measured rates of $O_2$ evolution in *Synechocystis* cells without addition (open circles) and in the presence of 5 mM histidine (open squares), as well as the rate of $O_2$ uptake, which reflects the rate of $^1O_2$ production (open triangles). The data are mean values from 3 measurements on independent biological samples with the indicated errors.

This result is highly important from the point of view of the light intensity dependence of photodamage. Experimental data demonstrate that the initial rate of photodamage linearly increases with light intensity even above the saturation of photosynthetic electron transport [61]. It has been argued that this finding can be explained only by assuming that photodamage of PSII is initiated by direct light induced inactivation of the Mn cluster of the water oxidizing complex [17,18]. The data, which were obtained earlier in isolated PSII membranes [56], and those presented here in intact *Synechocystis* cells demonstrate that the charge recombination mechanism of photodamage, in which $^3$P680 mediated $^1O_2$ production is a key event, can also explain the linear light intensity dependence of photoinhibition in a wide light intensity range, which extends well above the saturation level photosynthesis.

It has been reported recently that in higher plants ΔpH dependent dissipation of absorbed light energy via the non-photochemical quenching (NPQ) mechanism decreases $^1O_2$ formation and partially protects against photodamage [62]. In cyanobacteria NPQ does not depend on ΔpH, but occurs via light induced conformational change of the so called orange carotenoid protein (OCP) [63]. Since OCP-dependent NPQ is induced when light intensity increases one could expect a retardation of $^1O_2$ production at the onset of light energy dissipation via NPQ. Our data did not indicate such a process in the investigated light intensity range, which might be due to the saturation of the OCP-dependent quenching effect at high light intensities, or to some other effect whose background is not clear at present. This interesting question could be investigated in future studies by using *Synechocystis* mutants in which the level and activity of OCP-dependent NPQ can be controlled.

The rate of $O_2$ uptake at 2300 μmol quanta $m^{-2}$ $s^{-1}$ is ca. 20 μmol $O_2$/mg Chl/h when measured in a *Synechocystis* cell suspension at 5 μg Chl/mL, corresponding to 5.6 μM Chl concentration (Fig 4B). In absolute terms this corresponds to 0.055 μmol $O_2$/L/s rate of changing in the level of dissolved $O_2$ in the suspension. Considering that in cyanobacteria PSII and PSI contains ca. 35 and 96 Chl molecules based on their crystal structures [64,65], respectively, and also that the ratio of PSI:PSII is ≈3 [66] the 5.6 μM total Chl corresponds to ≈17 nM PSII concentration. In comparison, 1 μM RB in cell free BG11 induces ca. 16 μmol $O_2$/L/s uptake rate at 2300 μmol quanta $m^{-2}$ $s^{-1}$ light intensity due to $^1O_2$ trapping by His (Fig. 1B). Although the $^1O_2$ producing efficiency of RB and Chl cannot be exactly compared due to their different absorption characteristics, from the above data we can conclude that under illumination with white light the overall $^1O_2$ producing efficiency of Chls in intact *Synechocystis* cells is ca. 0.06% that of RB when equal number of sensitizing molecules are considered. However, if we consider whole PSII units as $^1O_2$ sensitizers and assume also that contribution of antenna Chls in PSI to the overall $^1O_2$ production is negligible in comparison to PSII, which is supported by EPR spin trapping measurements [67], we obtain that one PSII complex can produce $^1O_2$ with ca. 20% efficiency of one RB molecule when identical white light illumination is used. Since the main source of $^1O_2$ production in PSII is expected to be $^3$P680 this represents very efficient $^1O_2$ formation in the heart of PSII.

### *3.4. $^1O_2$ production and photodamage are correlated, and modulated by the efficiency of nonradiative charge recombination in the PSII reaction center*

It has been show earlier that the amino acid residue at the 130th position of the D1 PSII reaction center subunit influences the redox potential of the primary electron acceptor Phe by modifying H-bonding interactions [68,69]. Higher plants have a Glu residue at this position,

whereas numerous cyanobacteria have multiple D1 protein forms, which have either D1-130Glu or D1-130Gln. The Glu residue occurs in the so called high light D1 forms, which are expressed under high light exposure, whereas Gln occurs in the so called low light D1 forms, which are expressed under low light exposure of the cells (see [70]). Studies with site directed mutants of *Synechocystis* 6803, which have the same D1 form with D1-Gln130 under both low and high light conditions have demonstrated that the replacement of Gln with Glu increases the midpoint redox potential of Phe by 33 mV, whereas the D1-Gln130Leu mutation decreases the $E_m$(Phe/Phe$^-$) by 74 mV [68]. Biophysical characterization of these mutants have revealed that the D1-Gln130Glu accelerates charge recombination of the $S_2Q_A^{-\bullet}$ state, whereas the D1-Gln130Leu slows it down [71,72]. These effects have been assigned to the modulation of the rate of nonradiative recombination pathway from the primary charge separated state $P680^{+\bullet}Phe^{-\bullet}$ [71,72]. It has also been suggested earlier that non-radiative charge recombination within PSII [73], and in particular from the singlet state of the primary radical pair $^1[P680^{+\bullet}Phe^{-\bullet}]$ acts as an important photoprotective pathway (indicated by $k_{rd}$ in Scheme 1A), which competes with $^3$P680 formation and the consequent $^1O_2$ production [4,16,72]. Although this hypothesis is well supported by various lines of experimental evidence, so far only preliminary data were reported about the comparison of $^1O_2$ production and photodamage in intact cyanobacterial cells [74].

Here we applied the His-mediated $O_2$ uptake assay of $^1O_2$ detection in the D1-Gln130Glu and D1-Gln130Leu mutants in which the non-radiative recombination pathway is enhanced and retarded, respectively, in parallel with the measurement of PSII photodamage. As shown in Fig. 5A the rate of His-mediated oxygen uptake is smaller in the D1-Gln130Glu mutant, and higher in the D1-Gln130Leu mutant as compared to the WT. In order to confirm that the different rates of oxygen uptake in the mutants reflect different rates of $^1O_2$ production the measurements were performed in the presence of $D_2O$, which increases the lifetime of $^1O_2$. As expected $D_2O$ increased the rate of $O_2$ uptake in both mutants and the WT (Fig. 5A) supporting its origin from singlet oxygen trapping.

This idea was further confirmed by the effect of $NaN_3$, which is a specific singlet oxygen quencher. Since $NaN_3$ partially inhibits oxygen evolution the $O_2$ uptake assay was performed after blocking oxygen evolution by DCMU. Addition of $NaN_3$ to DCMU treated cells drastically decreased the His-mediated $O_2$ uptake, which supports further the correlation of $^1O_2$ production with $O_2$ uptake in the presence of His. The residual rate of $O_2$ uptake in the presence of $NaN_3$ may arise from the inability of $NaN_3$ to react with all $^1O_2$, which is accessible to His, or could reflect His oxidation by other ROS forms than $^1O_2$. The extent of His-dependent $O_2$ uptake, which can be quenched by $NaN_3$ is significantly higher in the D1-Gln130Leu than in the D1-Gln130Glu mutant, whereas the WT rate shows an intermediate level (Fig. 5A). These data confirm that the D1-Gln130Leu mutant produces $^1O_2$ at a significantly higher rate than the D1-Gln130Glu mutant, while the WT shows an intermediate rate.

Fig. 5A also shows that the rate of $O_2$ uptake due to His-mediated $^1O_2$ trapping is smaller in the presence of DCMU than without addition. It has been shown earlier that binding of electron transport inhibitors to the $Q_B$ site shifts the redox potential of $Q_A$ [51,75]. In case of DCMU $E_m(Q_A/Q_A^-)$ is shifted by +50 mV [51], which increases the free energy gap between $P680^+Phe^{-\bullet}$ and $P680^+Q_A^{-\bullet}$. As a consequence reverse electron transfer from the $P_{680}^{+\bullet}Q_A^{-\bullet}$ charge separated state to $^3[P680^{+\bullet}Phe^{-\bullet}]$ is thermodynamically disfavored and its rate decreases at the expense of direct recombination ($k_{rd}$ in Scheme 1A), which decreases the probability of $^3$P680 and $^1O_2$ formation (see Refs. [51,52]). This prediction has been validated earlier by EPR detection of $^1O_2$ in isolated PSII membranes [24,56], and supported further by our data in intact cells.

When susceptibility to photoinhibitory damage of PSII electron transport was measured in the presence of the protein synthesis inhibitor lincomycin, which prevents protein synthesis dependent repair of PSII, the D1-Gln130Glu cells were less inhibited than the WT (Fig. 5B). In contrast, the D1-Gln130Leu cells were damaged to a larger extent than either the D1-Gln130Glu, or the WT cells. This shows that the D1-Gln130Glu amino acid replacement provides protection against photodamage, while the D1-Gln130Leu replacement enhances it. It is very important to note that the extent of photodamage is correlated with the rate of $^1O_2$ production. Since the replacement of D1-Gln130 with Glu accelerates the efficiency of nonradiative charge recombination from the $^1[P680^{+\bullet}Phe^{-\bullet}]$ charge separated state, while the Leu replacement slows it down [72]these data provide further support for the earlier proposed [16,73] protective role of nonradiative charge recombination against $^1O_2$ mediated photodamage.

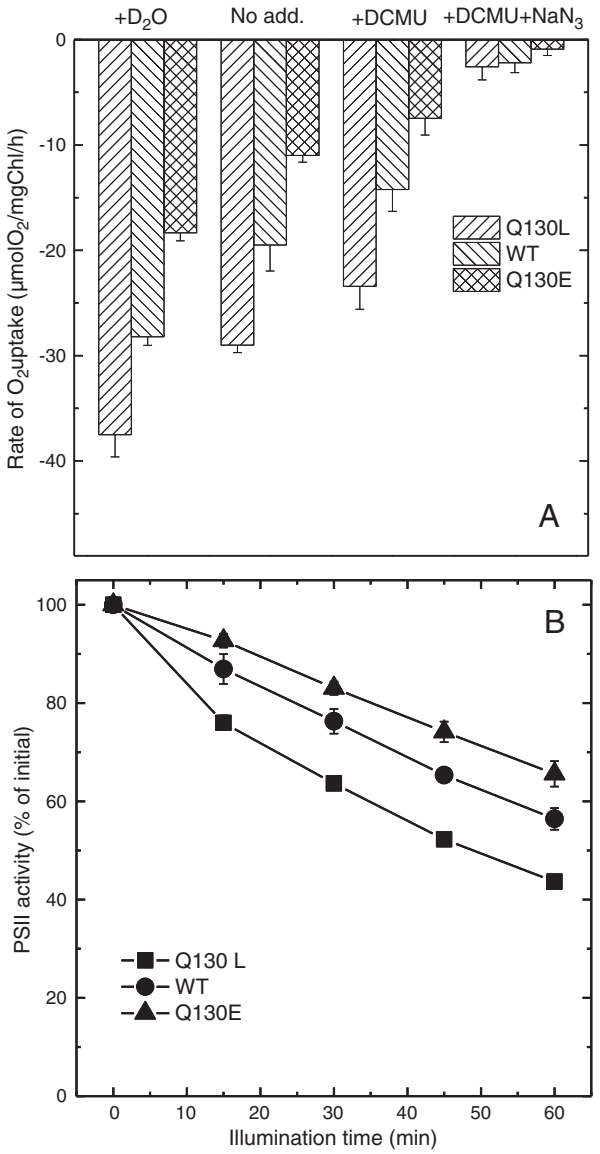


**Fig. 5.** The effect of D1-Gln130Glu and D1-Gln130Leu mutations on singlet oxygen production and photodamage in Synechocystis cells. A, $^1O_2$ production was assessed by measuring the rate by His-mediated oxygen uptake in WT, D1-Gln130Glu and D1-Gln130Leu *Synechocystis* strains. The measurements were performed using $H_2O$ or $D_2O$ in the BG-11 medium without further addition, or in the presence of 10 μM DCMU with or without 10 mM $NaN_3$. B, Light induced damage of PSII activity was assessed by measuring the rate of $O_2$ evolution in the presence of 0.5 mM DMBQ as artificial electron acceptor during exposure of WT (circles), D1-Gln130Glu (triangles) and D1-Gln130Leu (squares) to illumination with 500 μmol quanta $m^{-2}$ $s^{-1}$ light intensity. The data represent mean values form three independent measurements using different cell cultures, with the indicated error.

### 3.5. Concluding remarks

Here we report a method for detection of $^1O_2$ production in intact *Synechocystis* cells by using histidine as a chemical $^1O_2$ trap. This method requires only a standard oxygen electrode and can be easily applied in a wide range of organisms, provided that the exogenously added His penetrates through the cell wall. Therefore, the measurement of His-mediated $O_2$ uptake can remove the serious bottleneck of $^1O_2$ detection in intact aquatic photosynthetic organisms, which is imposed by the lack of EPR, or fluorescencent $^1O_2$ sensors that can readily penetrate the cell wall of cyanobacteria or algae. By applying this method we show that singlet oxygen production is linearly dependent on light intensity even above the saturation of photosynthesis. This finding provides further evidence that the experimentally observed linear light intensity dependence of the rate of photoinhibition [61] can be explained by $^1O_2$-mediated photodamage of PSII in agreement with earlier results obtained in isolated PSII membranes [56].

Our data also show that in the D1-Gln130Glu mutant, in which nonradiative charge recombination of the primary radical pair state is enhanced $^1O_2$ production is decreased, which effect is accompanied by decreased photodamage. In contrast, increased $^1O_2$ production concomitant with enhanced photodamage is observed in the D1-Gln130Leu mutant, in which nonradiative charge recombination of the primary radical pair state is enhanced. These data support the mechanism of photoinhibition in which $^1O_2$ production via interaction with $^3$P680 is a key step of PSII photodamage. The presented data provide support also for the hypothesis that nonradiative charge recombination of the singlet primary radical pair state provides photoprotection via competition with $^3$P680 and subsequent $^1O_2$ formation.

Supplementary data to this article can be found online at http://dx.doi.org/10.1016/j.bbabio.2013.02.016.

## Acknowledgements

This work was supported by the Hungarian granting agency OTKA (K-101433), the EU FP7 Marie Curie Initial Training Network HARVEST (project no. 238017), as well as by the TÁMOP-4.2.2.A-11/1/KONV-2012-0047 project. The authors are thankful for useful discussions with Prof. Éva Hideg and Dr. Zsuzsanna Deák.

## References

[1] N. Adir, H. Zer, S. Shochat, I. Ohad, Photoinhibition—a historical perspective, Photosynth. Res. 76 (2003) 343–370.
[2] E.-M. Aro, I. Virgin, B. Andersson, Photoinhibition of Photosystem II. Inactivation, protein damage and turnover, Biochim. Biophys. Acta 1143 (1993) 113–134.
[3] E. Tyystjarvi, Photoinhibition of Photosystem II and photodamage of the oxygen evolving manganese cluster, Coord. Chem. Rev. 252 (2008) 361–376.
[4] I. Vass, Role of charge recombination processes in photodamage and photoprotection of the photosystem II complex, Physiol. Plant. 142 (2011) 6–16.
[5] I. Vass, Molecular mechanisms of photodamage in the Photosystem II complex, Biochim. Biophys. Acta 1817 (2012) 209–217.
[6] N. Murata, S.I. Allakhverdiev, Y. Nishiyama, The mechanism of photoinhibiton *in vivo*: re-evaluation of the roles of catalase, α-tocopherol, non-photochemical quenching, and electron transport, Biochim. Biophys. Acta 1817 (2012) 1127–1133.
[7] I. Ohad, A. Berg, S.M. Berkowicz, A. Kaplan, N. Keren, Photoinactivation of photosystem II: is there more than one way to skin a cat? Physiol. Plant. 142 (2011) 79–86.
[8] I. Ohad, D.J. Kyle, C.J. Arntzen, Membrane protein damage and repair: removal and replacement of inactivated 32-kilodalton polypeptides in chloroplast membranes, J. Cell Biol. 99 (1984) 481–485.
[9] F.J.E. Van Mieghem, W. Nitschke, P. Mathis, A.W. Rutherford, The influence of the quinone-iron electron aaceptor complex on the reaction centre photochemistry of Photosystem II, Biochim. Biophys. Acta 977 (1989) 207–214.
[10] I. Setlik, S.I. Allakhverdiev, L. Nedbal, E. Setlikova, V.V. Klimov, Three typas of Photosystem II photoinactivation. I. Damaging processes on the acceptor side, Photosynth. Res. 23 (1990) 39–48.
[11] I. Vass, S. Styring, T. Hundal, A. Koivuniemi, E.-M. Aro, B. Andersson, Reversible and irreversible intermediates during photoinhibition of Photosystem II: stable reduced $Q_A$ species promote chlorophyll triplet formation, Proc. Natl. Acad. Sci. U. S. A. 89 (1992) 1408–1412.
[12] A.W. Rutherford, D.R. Paterson, J.E. Mullet, A light-induced spin-polarized triplet detected by EPR in Photosystem II reaction centers, Biochim. Biophys. Acta 635 (1981) 205–214.
[13] N. Keren, A. Berg, P.J.M. van Kan, H. Levanon, I. Ohad, Mechanism of Photosystem II photoinactivation and D1 protein degradation at low light: the role of back electron flow, Proc. Natl. Acad. Sci. U. S. A. 94 (1997) 1579–1584.
[14] A. Szilárd, L. Sass, É. Hideg, I. Vass, Photoinactivation of Photosystem II by flashing light, Photosynth. Res. 84 (2005) 15–20.
[15] É. Hideg, C. Spetea, I. Vass, Singlet oxygen and free radical production during acceptor- and donor-side-induced photoinhibition. Studies with spin trapping EPR spectroscopy, Biochim. Biophys. Acta 1186 (1994) 143–152.
[16] I. Vass, K. Cser, Janus-faced charge recombinations in photosystem II photoinhibition, Trends Plant Sci. 14 (2009) 200–205.
[17] M. Hakala, I. Tuominen, M. Keranen, T. Tyystjarvi, E. Tyystjarvi, Evidence for the role of the oxygen-evolving manganese complex in photoinhibition of Photosystem II, Biochim. Biophys. Acta 1706 (2005) 68–80.
[18] N. Ohnishi, S.I. Allakhverdiev, S. Takahashi, S. Higashi, M. Watanabe, Y. Nishiyama, N. Murata, Two-step mechanism of photodamage to Photosystem II: step 1 occurs at the oxygen-evolving complex and step 2 occurs at the photochemical reaction center, Biochemistry 44 (2005) 8494–8499.
[19] A. Boussac, J.-J. Girerd, A.W. Rutherford, Conversion of the spin state of the manganese complex in Photosystem II induced by near-infrared light, Biochemistry 35 (1996) 6984–6989.
[20] A. Telfer, S.M. Bishop, D. Phillips, J. Barber, Isolated photosynthetic reaction center of Photosystem II as a sensitizer for the formation of singlet oxygen. Detection and quantum yield determination using a chemical trapping technique, J. Biol. Chem. 269 (1994) 13244–13253.
[21] A.N. Macpherson, A. Telfer, J. Barber, T.G. Truscott, Direct detection of singlet oxygen from isolated Photosystem II reaction centres, Biochim. Biophys. Acta 1143 (1993) 301–309.
[22] A. Telfer, T.C. Oldham, D. Phillips, J. Barber, Singlet oxygen formation detected by near-infrared emission from isolated photosystem II reaction centres: direct correlation between P680 triplet decay and luminescence rise kinetics and its consequences for photoinhibition, J. Photochem. Photobiol. B 48 (1999) 89–96.
[23] É. Hideg, C. Spetea, I. Vass, Singlet oxygen production in thylakoid membranes during photoinhibition as detected by EPR spectroscopy, Photosynth. Res. 39 (1994) 191–199.
[24] C. Fufezan, C.M. Gross, M. Sjödin, A.W. Rutherford, A. Krieger-Liszkay, Influence of the redox potential of the primary quinone electron acceptor on photoinhibition in Photosystem II, J. Biol. Chem. 282 (2007) 12492–12502.
[25] B.B. Fischer, R.I.L. Eggen, A. Trebst, A. Krieger-Liszkay, The glutathione peroxidase homologous gen Gpxh in *Chlamydomonas reinhardtii* is upregulated by singlet oxygen produced in photosystem II, Planta 223 (2006) 583–590.
[26] É. Hideg, Zs. Deák, M. Hakala-Yatkin, M. Karonen, A.W. Rutherford, E. Tyystjarvi, I. Vass, A. Krieger-Liszkay, Pure forms of the singlet oxygen sensors TEMP and TEMPD do not inhibit Photosystem II, Biochim. Biophys. Acta 1807 (2011) 1658–1661.
[27] T. Tomo, H. Kusakabe, R. Nagao, H. Ito, A. Tanaka, S. Akimoto, M. Mimuro, S. Okazaki, Luminescence of singlet oxygen in photosystem II complexes isolated from cyanobacterium *Synechocystis* sp. PCC6803 containing monovinyl or divinyl chlorophyll *a*, Biochim. Biophys. Acta 1817 (2012) 1299–1305.
[28] É. Hideg, T. Kálai, K. Hideg, I. Vass, Photoinhibition of photosynthesis in vivo results in singlet oxygen production. Detection via nitroxide-induced fluorescence quenching in broad bean leaves, Biochemistry 37 (1998) 11405–11411.
[29] É. Hideg, P.B. Kós, I. Vass, Photosystem II damage induced by chemically generated singlet oxygen in tobacco leaves, Physiol. Plant. 131 (2007) 33–40.
[30] C. Flors, M.J. Fryer, J. Waring, B. Reeder, U. Bechtold, P.M. Mullineaux, S. Nonell, M.T. Wilson, N.R. Baker, Imaging the production of singlet oxygen *in vivo* using a new fluorescent sensor, Singlet Oxygen Sensor Greenr®, J. Exp. Bot. 57 (2006) 1725–1734.
[31] H. Li, T.B. Melo, J.B. Arellano, K.R. Naqvi, Temporal profile of the singlet oxygen emission endogenously produced by photosystem II reaction centre in an aqueous buffer, Photosynth. Res. 112 (2012) 75–79.
[32] R.K. Sinha, J. Komenda, J. Knoppová, M. Sedlárová, P. Pospísil, Small CAB-like proteins prevent formation of singlet oxygen in the damaged photosystem II complex of the cyanobacterium *Synechocystis* sp. PCC 6803, Plant Cell Environ. 35 (2012) 806–818.
[33] X. Ragás, A. Jiménez-Banzo, D. Sànchez-García, X. Batllori, S. Nonell, Singlet oxygen photosensitisation by the fluorescent probe Singlet Oxygen Sensor Green®, Chem. Commun. 45 (2009) 2920–2922.
[34] P.J. Nixon, T. Trost, B.A. Diner, Role of the carboxy terminus of polypeptide D1 in the assembly of a functional water-oxidizing manganese cluster in Photosystem II of the cyanobacterium *Synechocystis* sp. PCC 6803: assembly requires a free carboxyl group at C-terminal position 344, Biochemistry 31 (1992) 10859–10871.
[35] M. Trtilek, D.M. Kramer, M. Koblizek, Dual-modulation LED kinetic fluorometer, J. Lumin. 72–74 (1997) 597–599.
[36] I. Vass, D. Kirilovsky, A.-L. Etienne, UV–B radiation-induced donor- and acceptor-side modifications of Photosystem II in the cyanobacterium *Synechocystis* sp. PCC 6803, Biochemistry 38 (1999) 12786–12794.
[37] J.M. McCord, I. Fridovich, Superoxide dismutase. An enzymic function for erythrocuprein (hemocuprein), J. Biol. Chem. 244 (1969) 6049–6055.
[38] C. Beauchamp, I. Fridovich, Superoxide dismutase: improved assays and an assay applicable to acrylamide gels, Anal. Biochem. 44 (1971) 276–287.
[39] J.B. Verlhac, A. Gaudemer, I. Kraljic, Water-soluble porphyrins and metalloporphyrins as photosensitizers in aerated aqueous solutions. I. Detection and determination of quantum yield of formation of singlet oxygen, Nouv. J. Chim. 8 (1984) 401–406.

[40] V.V. Agon, W.A. Bubb, A. Wright, C.L. Hawkins, M.J. Davies, Sensitizer-mediated photooxidation of histidine residues: evidence for the formation of reactive side-chain peroxides, Free Radic. Biol. Med. 40 (2006) 698–710.
[41] J. Méndez-Hurtado, R. López, D. Suárez, M.I. Menéndez, Theoretical study of the oxidation of histidine by singlet oxygen, Chem. Eur. J. 18 (2012) 8437–8447.
[42] R.D. Hall, C.F. Chignell, Steady-state near-infrared detection of singlet molecular oxygen: a Stern–Volmer quenching experiment with sodium azide, Photochem. Photobiol. 45 (1987) 459–464.
[43] P.R. Ogilby, C.S. Foote, Chemistry of singlet oxygen. 36. Singlet molecular oxygen ($^1\Delta_g$) luminescence in solution following pulsed laser excitation. Solvent deuterium isotope effects on the lifetime of singlet oxygen, J. Am. Chem. Soc. 104 (1982) 2069–2070.
[44] S.Yu. Egorov, V.F. Kamalov, N.I. Koroteev, A.A. Krasnovsky Jr., B.N. Toleutaev, S.V. Zinukov, Rise and decay kinetics of photosensitized singlet oxygen luminescence in water. Measurements with nanosecond time-correlated single photon counting technique, Chem. Phys. Lett. 163 (1989) 421–424.
[45] J. Baier, M. Maier, R. Engl, M. Landthaler, W. Bäumler, Time-resolved investigations of singlet oxygen luminescence in water, in phosphatidylcholine, and in aqueous suspensions of phosphatidylcholine or HT29 cells, J. Phys. Chem. 109 (2005) 3041–3046.
[46] R. de Wijn, H.J. van Gorkom, Kinetics of electron transfer from $Q_A$ to $Q_B$ in Photosystem II, Biochemistry 40 (2001) 11912–11922.
[47] A.W. Rutherford, A.R. Crofts, Y. Inoue, Thermoluminescence as a probe of Photosystem II photochemistry: the origin of the flash-induced glow peaks, Biochim. Biophys. Acta 682 (1982) 457–465.
[48] H.H. Robinson, A. Crofts, Kinetics of the oxidation-reduction reactions of the Photosystem II quinone acceptor complex, and the pathway for deactivation, FEBS Lett. 153 (1983) 221–226.
[49] G. Forti, P. Gerola, Inhibition of photosynthesis by azide and cyanide and the role of oxygen in photosynthesis, Plant Physiol. 59 (1977) 859–862.
[50] T.M. Kana, Oxygen cycling in cyanobacteria with specific reference to oxygen protection in *Trichodesmium* spp. in: E.J. Carpenter, et al., (Eds.), Marine Pelagic Cyanobacteria: Trichodesmium and other Diazotrophs, Kluwer Academic Publishers, The Netherlands, 1992, pp. 29–41.
[51] A. Krieger-Liszkay, A.W. Rutherford, Influence of herbicide binding on the redox potential of the quinone acceptor in Photosystem II.: relevance to photodamage and phytotoxicity, Biochemistry 37 (1998) 17339–17344.
[52] A.W. Rutherford, A. Krieger-Liszkay, Herbicide-induced oxidative stress in Photosystem II, TIBS 26 (2001) 648–653.
[53] L.A. del Rio, V.C. Fernández, F.L. Rupérez, L.M. Sandalio, J.M. Palma, NADH induces the generation of superoxide radicals in leaf peroxisomes, Plant Physiol. 89 (1989) 728–731.
[54] A. Krieger-Liszkay, Singlet oxygen production in photosynthesis, J. Exp. Bot. 56 (2005) 337–346.
[55] A. Krieger-Liszkay, C. Fufezan, A. Trebst, Singlet oxygen production in photosystem II and related protection mechanism, Photosynth. Res. 98 (2008) 551–564.
[56] C. Fufezan, A.W. Rutherford, A. Krieger-Liszkay, Singlet oxygen production in herbicide-treated Photosystem II, FEBS Lett. 532 (2002) 407–410.
[57] A.W. Rutherford, Photosystem II, the water-splitting enzyme, Trends Biochem. Sci. 14 (1989) 227–232.
[58] A.J. Hoff, Magnetic field effects on photosynthetic reactions, Q. Rev. Biophys. 14 (1981) 599–665.
[59] F. van Mieghem, K. Brettel, B. Hillmann, A. Kamlowski, A.W. Rutherford, E. Schlodder, Charge recombination reactions in Photosystem II. 1. yields, recombination pathways, and kinetics of the primary pair, Biochemistry 34 (1995) 4798–4813.
[60] G.H. Schatz, H. Brock, A.R. Holzwarth, Picosecond kinetics of fluorescence and absorbance changes in Photosystem II particles excited at low photon density, Proc. Natl. Acad. Sci. U. S. A. 84 (1987) 8414–8418.
[61] E. Tyystjarvi, E.M. Aro, The rate constant of photoinhibition, measured in lincomycin-treated leaves, is directly proportional to light intensity, Proc. Natl. Acad. Sci. U. S. A. 93 (1996) 2213–2218.
[62] T. Roach, A. Krieger-Liszkay, The role of the PsbS protein in the protection of photosystems I and II against high light in *Arabidopsis thaliana*, Biochim. Biophys. Acta 1817 (2012) 2158–2165.
[63] A. Wilson, G. Ajlani, J.-M. Verbavatz, I. Vass, C.A. Kerfeld, D. Kirilovsky, A soluble carotenoid protein involved in phycobilisome-related energy dissipation in cyanobacteria, Plant Cell 18 (2006) 992–1007.
[64] J. Umena, K. Kawakami, J.-R. Shen, N. Kamiya, Crystal structure of oxygen-evolving photosystem II at a resolution 1.9 Å, Nature 473 (2010) 55–60.
[65] P. Jordan, P. Fromme, H.T. Witt, O. Klukas, W. Saenger, N. Krauβ, Three-dimensional structure of cyanobacterial photosystem I at 2.5 Å resolution, Nature 411 (2001) 909–917.
[66] K. Aizawa, T. Shimizu, T. Hiyama, K. Satoh, Y. Nakamura, Y. Fujita, Changes in composition of membrane-proteins accompanying the regulation of PS-I/PS-II stoichiometry observed with *Synechocystis* PCC 6803, Photosynth. Res. 32 (1992) 131–138.
[67] É. Hideg, I. Vass, Singlet oxygen is not produced in Photosystem I under photoinhibitory conditions, Photochem. Photobiol. 62 (1995) 949–952.
[68] S.A.P. Merry, P.J. Nixon, L.M.C. Barter, M. Schilstra, G. Porter, J. Barber, Modulation of quantum yield of primary radical pair formation in Photosystem II by site-directed mutagenesis affecting radical cations and anions, Biochemistry 37 (1998) 17439–17447.
[69] B. Loll, M. Broser, P.B. Kós, J. Kern, J. Biesiadka, I. Vass, W. Saenger, A. Zouni, Modeling of variant copies of subunit D1 in the structure of photosystem II from *Thermosynechococcus elongatus*, Biol. Chem. 389 (2008) 609–617.
[70] P.B. Kós, Zs. Deák, O. Cheregi, I. Vass, Differential regulation of *psbA* and *psbD* gene expression, and the role of the different D1 protein copies in the cyanobacterium *Thermosynechococcus elongatus* BP-1, Biochim. Biophys. Acta 1777 (2008) 74–83.
[71] F. Rappaport, M. Guergova-Kuras, P.J. Nixon, B.A. Diner, J. Lavergne, Kinetics and pathways of charge recombination in Photosystem II, Biochemistry 41 (2002) 8518–8527.
[72] K. Cser, I. Vass, Radiative and non-radiative charge recombination pathways in Photosystem II studied by thermoluminescence and chlorophyll fluorescence in the cyanobacterium *Synechocystis* 6803, Biochim. Biophys. Acta 1767 (2007) 233–243.
[73] I. Ohad, H. Raanan, N. Keren, D. Tchernov, A. Kaplan, Light-induced changes within Photosystem II protects *Microcoleus* sp. in biological desert sand crusts against excess light, PLoS One 5 (2010) e11000.
[74] K. Cser, I. Vass, Regulation of photoprotection by non-radiative charge recombination in Photosystem II, in: J.F. Allen, E. Gantt, J.H. Golbeck, B. Osmond (Eds.), Photosynthesis: Energy from the Sun, Springer, P.O. Box 17, 3300 AA Dordrecht, The Netherlands, 2008, pp. 47–50.
[75] I. Vass, S. Demeter, Classification of photosystem II inhibitors by thermodynamic characterization of thermoluminescence of inhibitor-treated chloroplasts, Biochim. Biophys. Acta 682 (1982) 496–499.